A comparison using two numerical approaches for modelling the impact of submarine landslides on suspended pipelines

Diponkar Saha[1], Bipul Hawlader[1], Sujan Dutta[2] & Ashutosh Dhar[1]
[1]*Memorial University of Newfoundland, St. John's, NL, Canada.*
[2]*Terraprobe, Brampton, ON, Canada.*

ABSTRACT
Submarine landslides could pose a significant threat to as-laid offshore pipelines. In the present study, numerical modelling is performed to study the impact of a clay block, which could be originated from a submarine landslide, on suspended pipelines in deep water environments. Two numerical approaches are used. In the coupled Eulerian–Lagrangian (CEL) approach in Abaqus FE software, the soil is modelled using the undrained shear strength of clay (s_u). In the computational fluid dynamics (CFD) approach of ANSYS CFX, the soft clay debris is modelled as a non-Newtonian fluid. In both approaches, the 'free water' (different from pore water) is modelled explicitly. Analyses are also performed without modelling the free water. It is shown that the free water in the cavity that forms behind the pipe during the flow of soil around it plays a significant role in the drag force. The developed numerical approaches in CEL and CFX can model the process of landslide impact; however, the CFX modelling is computationally efficient compared to the simulations with Abaqus CEL.

RÉSUMÉ
Les glissements de terrain sous-marins pourraient constituer une menace importante pour les pipelines offshore tels que posés. Dans la présente étude, une modélisation numérique est réalisée pour étudier l'impact d'un bloc d'argile, qui pourrait provenir d'un glissement de terrain sous-marin (débris), sur des pipelines suspendus dans des environnements en eau profonde. Deux approches numériques sont utilisées. Dans l'approche couplée Euler-Lagrangien (CEL) dans le logiciel Abaqus FE, le sol est modélisé en utilisant la résistance au cisaillement non drainé de l'argile (s_u). Dans l'approche de la dynamique des fluides computationnelle (CFD) dans ANSYS CFX, les débris d'argile molle sont modélisés comme un fluide non newtonien. Dans les deux approches, l'eau libre (différente de l'eau interstitielle) est modélisée explicitement. Les analyses sont également réalisées sans modélisation de l'eau libre. Il est montré que l'eau libre dans la cavité qui se forme derrière le tuyau pendant l'écoulement du sol autour de lui joue un rôle important dans la force de traînée. Les approches numériques développées en CEL et CFX peuvent modéliser le processus d'impact des glissements de terrain; cependant, la modélisation CFX est efficace par rapport aux simulations avec Abaqus CEL.

1 INTRODUCTION

Many small to large-scale landslides occur in offshore environments. A failed soil mass that generates from a submarine landslide might travel a large distance over the seafloor. Generally, offshore slopes are mild; a typical slope angle is less than 10°, except for some locally steep slope areas (Hadj-Hamou and Kavazanjian 1985, Dey et al. 2016). One of the major submarine landslides in Canadian history is the Grand Banks landslide of 1929, which involved transportation of 100–150 km^3 of sediments and damaged several transatlantic telegraph cables that were located hundreds of kilometers downslope from the place where the failure was initiated (Piper et al. 1988, 1999, Fine et al. 2005). The occurrence of many other submarine landslides has been reported in the literature (Piper et al. 1988, 1999, Bondevik et al. 2005, De Blasio et al. 2005, Masson et al. 2006).

Offshore pipelines are generally laid on the seafloor in deepwater environments (depth >400 m) and might penetrate into the soft clay seabed because of their weight, installation and hydrodynamic effects. When a pipeline is laid on an uneven seabed, a section of the pipeline might be suspended between two high points. A suspended pipeline might be affected by a failed seabed sediment that originates from a submarine landslide.

Arnold (1967) reported that, out of the 271 pipeline failures in the Mississipi delta during 1958–1965, approximately 55% of the pipeline failures were due to soil movements. Demar et al. (1977) showed that ~20% of the 125 pipeline failures in the Gulf of Mexico from 1971 to 1975 were also caused by soil movement. Therefore, proper estimation of pipeline drag force resulting from soil movement is one of the design requirements for offshore pipeline design.

The present study focuses on modelling the impact force of a clay block originating from a submarine landslide on a suspended pipeline. Experimental, analytical and numerical studies were conducted in the past for an estimation of drag force. The experimental works include small-scale laboratory tests and centrifuge tests, where a relative displacement between a section of pipe and surrounding soil was applied and the resistance of the soil was measured (Paulin et al., 1998; Phillips et al., 2004; Sahdi et al. 2014). Zakeri et al. (2009) conducted a series of flume tests to study the impact of clay-rich debris on suspended pipelines. Chi (2012) conducted centrifuge tests where a clay block

struck on a pipeline perpendicular to its direction of movement, at a wide range of impact velocities.

Zakeri (2009c) summarized the various approaches commonly used to estimate drag force on pipelines or piles. Two approaches are used to calculate the drag force: a geotechnical approach and a fluid mechanics approach. In the geotechnical approach, the drag force is proportional to the undrained shear strength (s_u) of the sliding clay block (e.g., Summers and Nyman 1985; Georgiadis 1991; Zhu and Randolph 2009). In the fluid mechanics approach, the soft debris is considered as a fluid and the drag force is proportional to the square of the impact velocity (Jiang and LeBlond 1993; Zakeri et al. 2008). Randloph and White (2012) proposed a combined geotechnical and fluid mechanics approach. The inertial component of drag force becomes significant when the impact velocity is high and/or debris shear strength is low (Sahdi et al. 2014; Dutta and Hawlader 2018).

Two types of numerical approaches could be used to calculate drag force: (i) large deformation finite element analysis and (ii) computational fluid dynamics approach. To determine the impact of a clay-rich debris on a suspended pipeline, two important numerical issues need to be resolved. First, what will be the interface behaviour as the debris engulfs the pipe which was initially surrounded by water? Second, when the debris flows around the pipe, a cavity forms behind it; whether this cavity has an influence on the drag force or the pipeline–soil interface behaviour can be simply modelled as bonded (full-tension)/unbonded (no-tension) and smooth/rough interface conditions, as commonly used in FE analysis. In the present study, these issues will be studied through numerical simulation of submarine landslide impacts on suspended pipelines, using a large deformation finite element modelling technique and a computational fluid dynamic approach.

2 PROBLEM STATEMENT

Figure 1 schematically shows three stages of the process of impact. A block of failed soil mass displaces in the downslope direction at a velocity v over the seabed (Fig. 1a). When it impacts a pipeline on its way, depending upon the location with respect to the seabed, the soil in the block might be displaced around the pipeline, as shown in Fig. 1(b). At this moment, the front part of the pipe is in contact with the soil. The force exerted by the failed soil mass is primarily due to penetration resistance, which is controlled by soil strength. Note that if the impact velocity is high, the inertial component also plays a significant role in the drag force (Sahdi et al. 2014; Dutta and Hawlader 2018). With a further displacement of the failed soil mass, the debris engulfs the pipe (Fig. 1(c)). However, a cavity behind the pipe will be formed, which might be connected to free water, and will be completely closed after a large displacement of the debris. The suction in the water-filled cavity would play a major role in the drag force (Dutta and Hawlader 2018).

Most of the existing large deformation finite element analyses for penetration resistance (vertical or lateral) have been conducted without considering the role of free water; the soil behaviour is modelled using the undrained shear strength and submerged unit weight. In addition, the pipe–soil interface is modelled as a fully bonded or unbonded condition. In the following sections, a FE modelling approach is presented where the role of free water and interface behaviour are examined by comparing the FE results with the results obtained from a computational fluid dynamics approach.

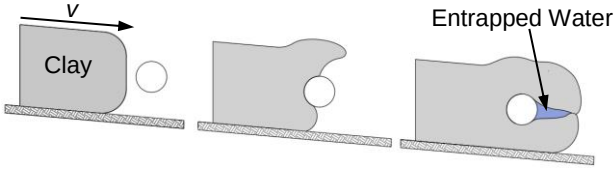

(a) Stage 1 (b) Stage 2 (c) Stage 3

Figure 1. Stages in submarine landslide impact on suspended pipelines

3 NUMERICAL MODELLING

3.1 Finite Element Modelling

The coupled Eulerian-Lagrangian approach available in Abaqus FE software is used for large deformation FE modelling. The details of numerical modelling, including its advantages and limitations, have been discussed in previous studies (Wang et al. 2015; Dutta et al. 2015). The size of the Eulerian domain (abcd in Fig. 2) is 4.35 m × 2.9 m (width × height). The seabed below this domain is considered as a rigid body. As the pipe is far from the seabed, the drag force will not be influenced by seabed behaviour. The soil is modelled as a Eulerian material. Since the Eulerian analysis allows only three-dimensional modelling, all the analyses are performed for a one-element thickness of 14.5 mm of the domain in the out-of-plane direction (i.e. along the axial direction of the pipe) to replicate a plane strain condition. The FE model comprises five parts: pipe, soil, water, void and seabed (Fig. 2).

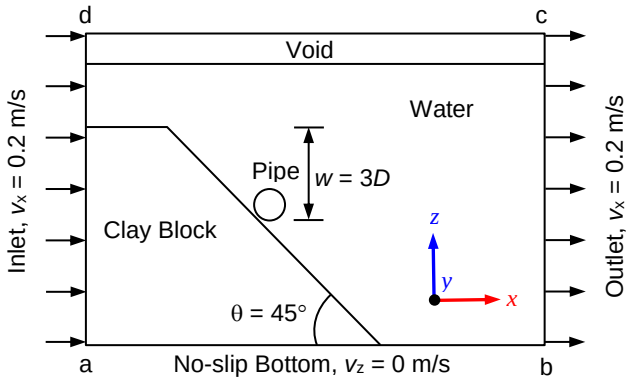

Figure 2. Details of FE modelling

The FE domain is discretized using EC3D8R elements in Abaqus, which is an 8-noded hexahedral linear brick, reduced integration Eulerian element with hourglass control. Fine mesh is used near the pipe. The thickness of the elements is ~15 mm near the pipe, which

is increased to 29 mm at a distance of five times of the diameter from the centre of the pipe, as shown in Fig. 3(a). Cubical elements of 29-mm length are used outside this zone.

The soil is modelled as elastic–perfectly plastic material, by defining the von Mises yield strength (= $2s_u$), where s_u is the undrained shear strength.

The free water is also modelled as a Eulerian material using a hydrodynamic material model by defining it in the form of the Mie-Grüneisen equation of state, which is available in Abaqus as a built-in model. Soil and free water are assigned in the domain by using the Eulerian Volume Fraction (EVF) tool—EVF equals 1 for Eulerian materials and 0 for the void.

Generally, in pipeline–soil interaction modelling, the pipeline is modelled as a Lagrangian body together with an appropriate contact definition for the interface. The currently available versions of Abaqus cannot simulate the bonding between the pipeline and surrounding soil/water, using full-tension interface conditions. However, bonding plays a significant role in drag force (Dutta and Hawlader 2018). The present study uses the following approach to simulate a fully bonded condition.

Instead of defining the pipe as a Lagrangian body, the pipe section (a circular hole of void) is extruded from the Eulerian body. The pipe surface is defined using a set of nodes on the wall. During the analysis, the velocity of these nodes is set to zero ($v_x = v_y = v_z = 0$); therefore, no Eulerian material can enter in the pipe—that is, the pipe surface behaves as an impermeable wall. Summing up the x-component of the nodal force of the nodes along the circumference of the pipe, the force on the pipe (F_x) is calculated.

The left and right boundaries of the domain are defined as an inlet and outlet, respectively. At the outlet, in addition to the velocity boundary condition, an equilibrium outflow boundary condition is used. This ensures the reduction of spurious reflection of the Eulerian materials at the outflow boundary. This boundary condition is used because the pressure distribution is unknown. A free-slip boundary condition is used for the interface between the seabed and debris/free water. All the out-of-plane vertical surfaces are assigned with a $v_y = 0$ boundary condition.

The numerical analysis is divided into two steps: gravitational loading and debris flow. In the first step, the gravity is applied gradually to achieve the in-situ stress condition of the soil and hydrostatic stress condition in the free water. In the second step, the debris block is forced to slide laterally to the right by applying a velocity boundary condition in the x-direction (v_0 = 0.2 m/s) at the inlet and outlet.

3.2 Finite Volume Modelling

ANSYS CFX software is used for the computational fluid dynamics analyses. The geometry and boundary conditions in CFX analysis are the same as for Abaqus CEL modelling, as discussed above. However, no void space is required above the water, as in CEL modelling, as shown in Fig. 3(b). The pipe is modelled as a wall with a no-slip boundary condition. Clay and water are modelled as multiphase homogenous Eulerian materials. The shear resistance of clay is defined using the dynamic viscosity, μ_d (= $s_u/\dot{\gamma}$, where $\dot{\gamma}$ is the shear strain rate), as a rigid-plastic non-Newtonian fluid. A constant dynamic viscosity of 8.9×10^{-7} kPa.s is used for water. Further details of CFX modelling are available in the work of Dutta and Hawlader (2018).

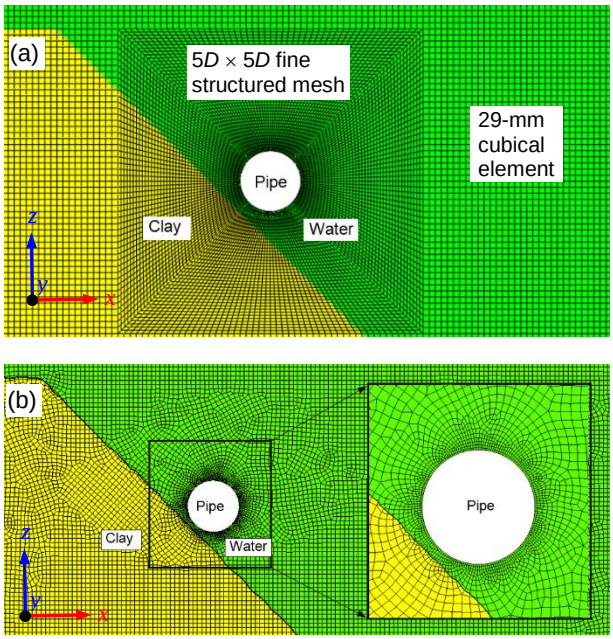

Figure 3. Mesh near the pipe: (a) Finite element (b) CFX

4 PARAMETER SELECTIONS

Table 1 shows the geometry and properties of clay and water used in this study. For FE analysis, the clay is modelled as an elastic-perfectly plastic material with an undrained Young's modulus of $500s_u$. Although the undrained shear strength of debris can vary with depth, it is assumed to be uniform (s_u = 5 kPa). Moreover, the effects of strain rate and strain softening on s_u are not considered in this study.

Table 1. Parameters used in numerical analyses

Pipe:	
Outer diameter, D_o	290 mm
Length, L	14.5 mm
Clay:	
Undrained shear strength, s_u	5 kPa
Undrained Young's modulus in FE analysis, E_u	$500s_u$
Undrained Poisson's ratio in FE analysis, ν_u	0.495
Saturated unit weight of soil, γ_{sat}	15.81 kN/m^3
Water in FE:	
Equation of State (EOS)	
Velocity of sound in water, c_0	1531 m/s
Slope of $U_s - U_p$ curve, s	0
Grüneisen ratio, Γ_0	0
Dynamic viscosity of water in CFX and FE analysis, μ_D	8.9×10^{-7} kPa.s

5 RESULTS

5.1 Force–Displacement Behaviour

Figure 4 shows the normalized force ($N = F_x/s_{uN}D_eL$) versus normalized lateral penetration ($\hat{u} = u/D_e$) curves obtained for FE and CFX simulations. Here, $s_{uN} = 2/\sqrt{3}s_u$, L = length of the pipe in the out-of-plane direction, $D_e = D_o + t_i$, where t_i is the average thickness of the soil elements just outside the pipe surface (please see Hawlader et al. 2015 and Dutta and Hawlader 2018 for further discussion). The lateral penetration distance at time t is calculated as $u = v_0(t-t_0)$, where t_0 is the time when the pipe touches the sloped surface and the force on the pipe starts to increase.

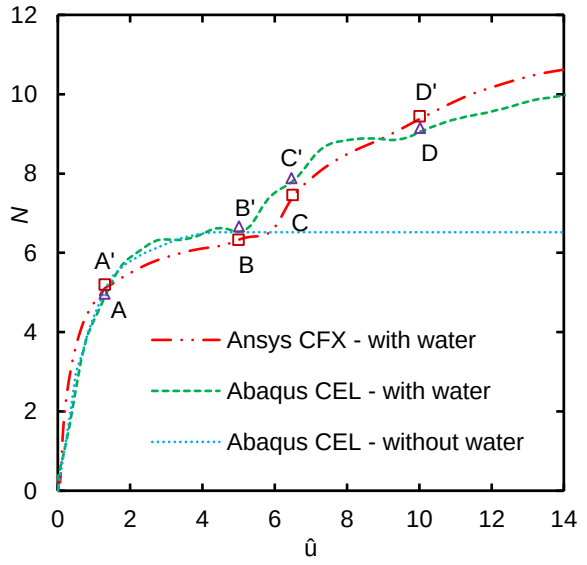

Figure 4. Normalized force–displacement curves

Figure 4 shows that N increases rapidly with $\hat{u}$ up to $\hat{u} \sim 2$; thereafter, the rate of increase of N is small. At $\hat{u}$ between 4 and 5, the normalized resistance is almost constant. (For points A, B, C, D see Fig. 5.) In both CFX and CEL analyses, the resistance again increases after $\hat{u} \sim 5$, which is because of the development of suction in the cavity that forms behind the pipe, as discussed in the following sections. For the analyses performed in this study, both CFX and CEL give similar force–displacement curves.

5.2 Computational cost

Similar to other large deformation finite element analyses, Abaqus CEL is computationally expensive. The CEL analysis presented in Fig. 4 took 51.5 hours with a Core™ i7-6700 CPU @ 3.40 GHz, 16.0 GB RAM desktop. For the same computer, the CFX analysis in Fig. 4 took only 5 hours. In other words, the modelling of a submarine landslide's impact on pipeline using ANSYS CFX is computationally efficient compared to Abaqus CEL analysis.

5.3 Soil Failure Mechanisms

Figure 5 shows the development of plastic shear strains ($\gamma_p = \int_0^t \dot{\gamma}\, dt$, where $\dot{\gamma}$ is shear strain rate and t is time) in the soil for different levels of penetration, as shown by open squares and triangles in Fig. 4 (please see Dutta et al. (2015) and Dutta and Hawlader (2018) for further details on plastic shear strain calculation). At 1.3D penetration, the plastic shear strain is mainly accumulated in front of the pipe (left side) (Figs. 5(a) and 5(b)). At 5D penetration, a considerable heave occurs above the pipe together with a large shear strain accumulation (Figs. 5(c) and 5(d)). At this time, a wide channel is formed behind the pipe (right side), which is filled with free water. As the channel is wide, free water can flow easily through it; therefore, the free water does not have any significant effect on the lateral force, and the force at this stage is primarily governed by the geotechnical resistance of clay. Some difference between soil failure and accumulated plastic shear strain obtained from CEL and CFX is potentially due to the difference in solution techniques used in these softwares for modelling of sediment. With an increase in penetration, the channel becomes smaller and, at $\hat{u} \sim 6$–7, it is almost closed in both CFX and CEL simulations (Figs. 5(e) & 5(f)). The length of closure increases with further penetration, and the cavity behind the pipe becomes almost isolated from the free water at $\hat{u} > 10$ ((Figs. 5(g) & 5(h)). When the channel becomes narrow or closes, a suction (i.e. total pressure is below the initial ambient pressure) generates in the water in the cavity, which influences the lateral resistance, as discussed in the following sections.

5.4 Role of Water in the Channel/Cavity behind the Pipe

The suction behind the pipe for two large penetration distances is shown in Fig. 6. In CFX, the pressure (p) is obtained for each time increment. The zone of water where p is less than the initial ambient pressure (defined as a reference pressure in the analysis) represents the area where suction is developed. In CEL, the initial ambient pressure is calculated at each location after the gravity step, which is defined as a state variable. Using a user subroutine, the suction is calculated by subtracting the initial ambient pressure from the current pressure. Note here that the negative pressure in the soil (outside the dashed line that represents the water-filled cavity in Fig. 6), can be viewed as the tension in soil elements.

Comparison between suction contours in Fig. 6 shows that, although the magnitude of suction is comparable in CEL and CFX simulations, there is a difference between the shape and size of the zone where suction is developed. This is primarily due to the modelling technique and especially the modelling of the soil–water interface. Because of this, the size/shape of the water-filled cavity is different, as shown in Fig. 5. However, as the magnitude of suction is comparable, the force–displacement curves are similar, as shown in Fig. 4.

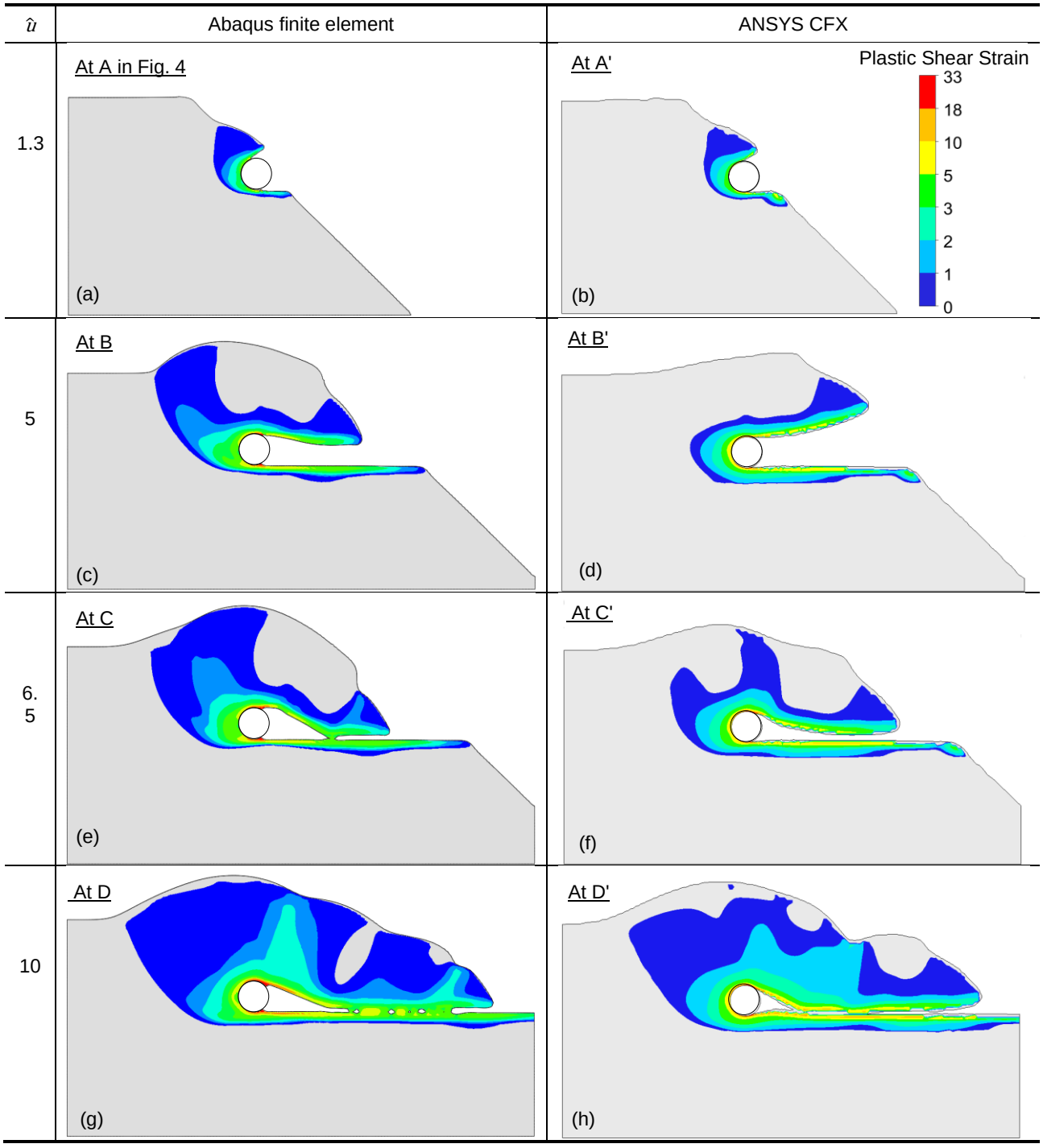

Figure 5. Development of plastic shear strain, γ_p and soil failure with penetration of the pipe

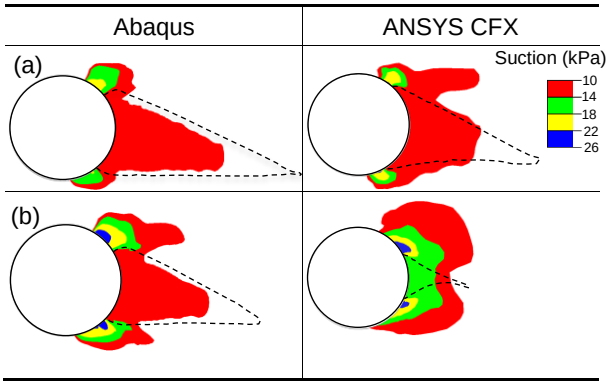

Figure 6. Comparison of suction around the pipe in Abaqus and Ansys CFX at: (a) $u = 10D$; (b) $u = 14D$

In pipeline–soil interaction modelling—for example, vertical and lateral resistance calculations—free water is not modelled explicitly as a separate phase. Instead, the soil is modelled using the submerged unit weight (γ') and pipe–soil interface is considered as having smooth/rough and fully-bonded/unbonded conditions (e.g. Martin and White 2012; Dutta et al. 2015). To show the advantages of free water modelling and effects of bonding, the following three sets of FE analyses are performed and the results compared with previous analyses. In Case-I, FE analysis is performed with a void only (instead of water as in Fig. 2) and γ' as the unit weight of the soil block. The fully bonded condition, as described above, is used. In Case-II, the pipe is modelled as a Lagrangian body where interface behaviour is defined as a smooth and rough condition, without bonding, while the other conditions are the same as in Case-I. The Case-III analyses are performed using Abaqus/Explicit for a wished-in-place pipe configuration for fully-bonded and unbonded together with smooth and rough interface conditions. For clarity, the force–displacement curve for Case-I only is shown in Fig. 4. For the other cases, the calculated maximum force is shown in Table 2.

Table 2. Maximum normalized resistance

Case No.	Interface behaviour		Maximum normalized force
Case-I	-	fully bonded	6.5
Case-II	smooth	unbonded	5.2
	rough	unbonded	5.9
Case-III	smooth	fully bonded	9.2
	rough	fully bonded	10.8
	smooth	unbonded	5.75
	rough	unbonded	6.5

Table 2 shows that the maximum normalized force for the unbonded cases is significantly lower than for the bonded cases. As expected, the lowest force is calculated with an unbonded and smooth pipeline–soil interface condition. The bonded behaviour could not be simulated properly in CEL without modelling free water explicitly; therefore, Case-I simulation gives a significantly lower maximum force than that shown in Fig. 4. For the cases analyzed in this study, the maximum force for Case-III with a fully bonded and rough interface condition is comparable to that in Fig. 4. Note, however, that the Case-III analyses are for a wished-in-place pipe configuration where a relatively small displacement is required to reach the maximum force, and the role of cavity and surface heave, as shown in Fig. 5, on drag force, is not modelled. Maximum normalised force of 6.4 is estimated using ALA and PRCI guidelines, which shows close agreement with the unbonded cases. But higher maximum normalised values than the guidelines are observed for fully bonded cases where soil–water–pipe interaction is considered.

5 CONCLUSIONS

Deepwater offshore pipelines are generally laid on the seafloor and can be either partially embedded or suspended. Suspended pipelines might interact with a submarine landslide-induced failed soil mass that can damage the pipeline. Proper estimation of pipe drag force is an important design parameter, which depends on many factors, including impact velocity, shear strength debris, pipeline–soil interface behaviour and free water. Dutta and Hawlader (2018) modelled this process, including the role of free water, using a computational fluid dynamics (CFD) approach. In the present study, it is shown that the coupled Eulerian-Lagrangian (CEL) approach of finite element analysis can be used to model this process. However, in CEL, free water and interface behaviour (e.g. bonding) should be modelled properly. Although the force–displacement behaviour obtained from CFD and CEL are comparable, the CFD modelling using ANSYS CFX is computationally efficient.

The simulations are performed for ideal soil (without considering strain rate and softening effects on undrained shear strength) and only one burial depth, pipe diameter and impact velocity. Further studies are required to investigate the effect of these parameters on drag force.

6 ACKNOWLEDGEMENTS

The work presented in this paper has been supported by the Research and Development Corporation of Newfoundland and Labrador through the ArcticTECH program, Petroleum Research Newfoundland and Labrador, Mitacs, and the Natural Sciences and Engineering Research Council of Canada (NSERC).

7 REFERENCES

American Lifelines Alliance. Guidelines for the design of buried steel pipe. *Federal Emergency Management Agency,* USA. 2001:75.

Arnold, K.E. 1967. Soil Movements and their Effects on Pipelines in the Mississippi Delta Region, Ph.D dissertation, Tulane University of Louisiana, New Orleans, Louisiana, USA.

Bondevik, S., Løvholt, F., Harbitz, C., Mangerud, J., Dawson, A. and Svendsen, J.I. 2005. The Storegga

Slide Tsunami—Comparing Field Observations with Numerical Simulations, *Marine and Petroleum Geology*, 25: 195–208.

Chi, K. F. 2012. Glide Block or Out-Runner Block Impact on Suspended Submarine Pipeline, MEng. thesis, Memorial University, St. John's, NL, Canada.

De Blasio, F.V., Elverhøi, A., Issler, D., Harbitz, C.B., Bryn, P. and Lien, R. 2005. On the Dynamics of Subaqueous Clay Rich Gravity Mass Flows—The Giant Storegga Slide, Norway, *Marine and Petroleum Geology*, 22(1–2): 179–186.

Demars, K.R., Nacci, V.A. and Wang, W.D. 1977. Pipeline Failure: A Need for Improved Analyses and Site Surveys, *Offshore Technology Conference*, Houston, Texas, USA, 28: 76–83.

Dey, R., Hawlader, B., Phillips, R. and Soga, K. 2016. Modeling of Large-Deformation Behaviour of Marine Sensitive Clays and its Application to Submarine Slope Stability Analysis. *Canadian Geotechnical Journal*, *53*(7): 1138–1155.

Dutta, S. and Hawlader, B. 2018. Pipeline–Soil–Water Interaction Modelling for Submarine Landslide Impact on Suspended Offshore Pipelines. *Géotechnique*,1–43.

Dutta, S., Hawlader, B. and Phillips, R. 2015. Vertical Penetration of Offshore Pipelines: A Comparative Study between Finite Element and Finite Volume Methods, *International Conference on Ocean, Offshore and Arctic Engineering*, ASME, pp. 0–10.

Fine, I.V., Rabinovich, A.B., Bornhold, B.D., Thomson, R.E. and Kulikov, E.A. 2005. The Grand Banks Landslide-Generated Tsunami of November 18, 1929: Preliminary Analysis and Numerical Modelling, *Marine Geology*, 215(1–2): 45–57.

Georgiadis, M. 1991. Landslide Drag Forces on Pipelines, *Soils and Foundations*, 31(1): 156–161.

Hadj-Hamou, T., and Kavazanjian, E., Jr. 1985. Seismic Stability of Gentle Infinite Slopes, *Journal of Geotechnical Engineering*, 111(6): 681–697.

Jiang, L. and LeBlond, P.H. 1993. Numerical Modelling of an Underwater Bingham Plastic Mudslide and The Waves which it Generates. *Journal of Geophysical Research*: *Oceans*, 98(C6): 10303–10317.

Martin, C.M. and White, D.J. 2012. Limit Analysis of the Undrained Bearing Capacity of Offshore Pipelines, Géotechnique, 62(9): 847–863.

Masson, D.G., Harbitz, C.B., Wynn, R.B., Pedersen, G. and Løvholt, F. 2006. Submarine Landslides: Processes, Triggers and Hazard Prediction, *Philosophical Transactions of the Royal Society of London A: Mathematical, Physical and Engineering Sciences*, 364(1845): 2009–2039.

Paulin, M.J., Phillips, R. and Boivin, R. 1996. An Experimental Investigation into Lateral Pipeline/Soil Interaction, *International Conference on Offshore Mechanics Arctic Engineering*, ASME, New York, USA.

Phillips, R., Nobahar, A. and Zhou, J. 2004. Trench Effects on Soil/Pipe Interaction, *Proceedings of the 2004 International Pipeline Conference*, New York, USA, ASME: 321–327.

Piper, D.J. 1988. The 1929 Grand Banks Earthquakes, Slump, and Turbidity Current. Geological Society of America, Special Paper, 229: 77–92.

Piper, D.J., Cochonat, P. and Morrison, M.L. 1999. The Sequence of Events around the Epicentre of the 1929 Grand Banks Earthquake: Initiation of Debris Flow and Turbidity Current Inferred from Sidescan Sonar, *Sedimentology*, 46(1): 79–97.

Randolph, M. F. and White, D. J. 2012. Interaction Forces Between Pipelines and Submarine Slides—A Geotechnical Viewpoint, *Ocean Engineering*, 48: 32–37.

Sahdi, F., Gaudin, C., White, D.J., Boylan, N. and Randolph, M.F. 2014. Centrifuge Modelling of Active Slide-Pipeline Loading in Soft Clay, *Géotechnique*, 64(1): 16–27.

Summers, P.B. and Nyman, D.J. 1985. An Approximate Procedure for Assessing the Effects of Mudslides on Offshore Pipelines, *Journal of Energy Resources Technology*, 107(4): 426–432.

Wang, D., Bienen, B., Nazem, M., Tian, Y., Zheng, J., Pucker, T., and Randolph, M. F. 2015. Large Deformation Finite Element Analyses in Geotechnical Engineering, *Computers and Geotechnics*, 65: 104–114.

Zakeri, A., Høeg, K. and Nadim, F. 2008. Submarine Debris Flow Impact on Pipelines—Part I: Experimental Investigation, *Coastal engineering*, 55(12): 1209–1218.

Zakeri, A. 2009c. Review of the State-of-the-Art: Drag Forces on Submarine Pipelines and Piles Caused by Landslide or Debris Flow Impact, *Journal of offshore mechanics and Arctic engineering*, ASCE, 131(1).

Zakeri, A., Hawlader, B. and Chi, K. 2012. Drag Forces Caused by Submarine Glide Block or Out-Runner Block Impact on Suspended (Free-Span) Pipelines. *Ocean Engineering*, 47: 50–57.

Zhu, H., and Randolph, M. F. 2009. Large Deformation Finite-Element Analysis of Submarine Landslide Interaction with Embedded Pipelines. *International Journal of Geomechanics*, 10(4): 145–152.